

# New Molecular Complexes of Fullerenes C<sub>60</sub> and C<sub>70</sub> with Tetraphenylporphyrins [M(tpp)], in which M = H<sub>2</sub>, Mn, Co, Cu, Zn, and FeCl

Dmitri V. Konarev,<sup>[a]</sup> Ivan S. Neretin,<sup>[b]</sup> Yuri L. Slovokhotov,<sup>[b]</sup> Evgeniya I. Yudanova,<sup>[a]</sup> Natal'ya V. Drichko,<sup>[c]</sup> Yuri M. Shul'ga,<sup>[a]</sup> Boris P. Tarasov,<sup>[a]</sup> Leonid L. Gumanov,<sup>[a]</sup> Andrei S. Batsanov,<sup>[d]</sup> Judith A. K. Howard,<sup>[d]</sup> and Rimma N. Lyubovskaya\*<sup>[a]</sup>

**Abstract:** New molecular complexes of fullerenes C<sub>60</sub> and C<sub>70</sub> with tetraphenylporphyrins [M(tpp)] in which M = H<sub>2</sub>, Mn<sup>II</sup>, Co<sup>II</sup>, Cu<sup>II</sup>, Zn<sup>II</sup> and Fe<sup>III</sup>Cl, have been synthesised. Crystal structures of two C<sub>60</sub> complexes with H<sub>2</sub>TPP, which differ only in the number of benzene solvated molecules, and C<sub>60</sub> and C<sub>70</sub> complexes with [Cu(tpp)] have been studied. The fullerene molecules form a honeycomb motif in H<sub>2</sub>TPP·2C<sub>60</sub>·3C<sub>6</sub>H<sub>6</sub>, puckered graphite-like layers in

H<sub>2</sub>TPP·2C<sub>60</sub>·4C<sub>6</sub>H<sub>6</sub>, zigzag chains in [Cu(tpp)]·C<sub>70</sub>·1.5C<sub>7</sub>H<sub>8</sub>·0.5C<sub>2</sub>HCl<sub>3</sub> and columns in [Cu(tpp)]<sub>2</sub>·C<sub>60</sub>. H<sub>2</sub>TPP has van der Waals contacts with C<sub>60</sub> through nitrogen atoms and phenyl groups. Copper atoms of the [Cu(tpp)] molecules are weakly coordinated with C<sub>70</sub>, but form no shortened contacts with C<sub>60</sub>.

**Keywords:** copper · fullerenes · porphyrinoids · structure elucidation

The formation of molecular complexes with fullerenes affects the ESR spectra of [M(tpp)] (M = Mn, Co and Cu). [Mn(tpp)] in the complex with C<sub>70</sub> lowers its spin state from  $S = 5/2$  to  $S = 1/2$ , whereas [Co(tpp)] and [Cu(tpp)] change the constants of hyperfine interaction. ESR, IR, UV-visible and X-ray photoelectron spectroscopic data show no noticeable charge transfer from the porphyrinate to the fullerene molecules.

## Introduction

Donor–acceptor complexes of fullerenes exhibit promising physical properties (superconductivity, and ferromagnetism)<sup>[1]</sup> and may be important for the study of photoinduced electron transfer.<sup>[2]</sup> To-date a great number of the molecular compounds with substituted tetrachalcogenafulvalenes,<sup>[3]</sup> cyclotrimeratrylenes,<sup>[4]</sup> calixarenes,<sup>[5]</sup> concave aromatic donors,<sup>[6]</sup> porphyrazine<sup>[7]</sup> and other molecules,<sup>[1b, 8]</sup> has been synthesised.

Fullerene complexes with porphyrins are of particular interest in several aspects, as their electronic structure can vary in a wide range, from co-crystals of essentially neutral, weakly interacting molecules, through charge-transfer complexes, to radical-ion salts. Thus, studies of photoinduced electron transfer in C<sub>60</sub> solutions containing octaethyl- or tetraphenylporphyrins, their Mg<sup>II</sup> and Zn<sup>II</sup> derivatives<sup>[9]</sup> and in dyad molecules with C<sub>60</sub> covalently bonded to porphyrins<sup>[10]</sup> show the formation of relatively long-lived charge-separated states. Hence the complexes of fullerenes with porphyrins in the solid state may be promising as photoactive materials for xerography and solar energy transducers. Some porphyrins can reduce C<sub>60</sub> to yield radical-ion salts, for example, chromium(II) tetraphenylporphyrin [Cr<sup>II</sup>(tpp)] reduces C<sub>60</sub> in toluene/tetrahydrofuran, giving air-sensitive [Cr<sup>III</sup>(tpp)<sup>+</sup>][C<sub>60</sub><sup>-</sup>]·3THF,<sup>[11]</sup> and tin(II) tetra-*p*-tolylporphyrin [Sn<sup>II</sup>(tptp)] can reduce C<sub>60</sub> in the presence of *N*-methylimidazole (*N*-MeIm) to form [Sn<sup>IV</sup>(tptp)(*N*-MeIm)<sub>2</sub>]<sup>2+</sup>(C<sub>60</sub><sup>-</sup>)<sub>2</sub>.<sup>[12]</sup> Since it is known that radical-ion salts of porphyrins with certain planar  $\pi$ -acceptors (e.g., manganese(II) tetraphenylporphyrin and tetracyanoethylene) have a one-dimensional ferromagnetic ordering at helium temperatures,<sup>[13]</sup> fullerenes may also prove useful as acceptor molecules in the design of new molecular magnetic materials.

On the other hand, molecular complexes can be important in building complex inclusion nanostructures, in which the

[a] Prof. R. N. Lyubovskaya, Dr. B. P. Tarasov, Dr. L. L. Gumanov, Dr. D. V. Konarev, Dr. E. I. Yudanova, Dr. Yu. M. Shul'ga  
Institute of Problems of Chemical Physics  
Russian Academy of Sciences  
Chernogolovka, Moscow Region 142432 (Russia)  
Fax: (+7)096-515-35-88  
E-mail: lyurn@icp.ac.ru

[b] I. S. Neretin, Dr. Yu. L. Slovokhotov  
Institute of Organoelement Compounds  
Russian Academy of Sciences  
28 Vavilov Str., Moscow 117334 (Russia)

[c] Dr. N. V. Drichko  
A.F. Ioffe Physical-Technical Institute  
St.-Petersburg 194021 (Russia)

[d] Dr. A. S. Batsanov, Prof. J. A. K. Howard  
Department of Chemistry, University of Durham  
South Road, Durham DH1 3LE (UK)  
Fax: (+44)191-384-4737  
E-mail: j.a.k.howard@durham.ac.uk

principal problem is to control weak, principally van der Waals, interactions. These effects can be also employed for separation and purification of fullerenes, for example, by using appended porphyrins as chromatographic materials.<sup>[14]</sup> Knowledge of the crystal structures of porphyrin–fullerene complexes can help to understand the porphyrin–fullerene interaction in a chromatographic column and to optimise the process.

Metal complexes with rigidly nonplanar (warped) macrocycles, such as tetra- and octamethyldibenzotetraaza[14]annulenes (TMTAA and OMTAA, respectively), have already proved useful in supramolecular chemistry.<sup>[15]</sup> They form a variety of complexes with globular molecules, including C<sub>60</sub> and C<sub>70</sub>, stabilised by the complementarity of curvature between host and guest, for example, a fullerene fitting into the concave surface of the metal-macrocycle complex. Since porphyrins also can adopt warped, as well as planar, conformations, they apparently can perform similar functions as [M<sup>II</sup>(tmtaa)] and [M<sup>II</sup>(omtaa)].

Recently, a series of molecular complexes of C<sub>60</sub> and C<sub>70</sub> with metal (Co<sup>II</sup>, Zn<sup>II</sup>, Ni<sup>II</sup>, Cu<sup>II</sup> and Fe<sup>III</sup>) derivatives of octaethylporphyrin (OEP) were synthesised.<sup>[16]</sup> However, all of them were found to contain planar, rather than warped, porphyrin systems. The crystal structure of a C<sub>60</sub> complex with octakis(dimethylamino)porphyrizine (ODMAP) was reported,<sup>[7]</sup> as well as the structures, ESR and magnetism of its metal derivatives, [Cu(odmap)]<sub>2</sub>·C<sub>60</sub>·2C<sub>6</sub>H<sub>6</sub> and [Ni(odmap)]·C<sub>60</sub>.<sup>[17]</sup> In the latter, a slightly concave (“dished”) conformation of [Cu(odmap)] contrasts with more warped, saddle-like conformation of [Ni(odmap)]. Eight structurally characterised complexes of C<sub>60</sub> or C<sub>70</sub> with tetraphenylporphyrin (H<sub>2</sub>TPP), its methylated derivatives and [M(tpp)], all contain practically planar porphyrin systems, closely packed with fullerene cages.<sup>[18]</sup> Thereupon Boyd et al. concluded that the

van der Waals attraction (dispersion forces) between the curved π surface of a fullerene and a planar π surface of a porphyrin is very favourable for a supramolecular recognition, without the necessity of matching a concave host with a complementary convex guest.<sup>[18]</sup> In view of these competing models, it is desirable to study a wider variety of fullerene-porphyrin combinations. It is also noteworthy, that the first characterised endohedral fullerene was stabilised in a complex with porphyrin, [Sc<sub>3</sub>N]@[C<sub>80</sub>][Co(oep)]·1.5CHCl<sub>3</sub>·0.5C<sub>6</sub>H<sub>6</sub>.<sup>[19]</sup>

We have already prepared molecular complexes of fullerenes with manganese(II) and cobalt(II) tetraphenylporphyrins, and their preliminary ESR study is reported elsewhere.<sup>[20]</sup> In this work we report the synthesis and characterisation of new molecular complexes of fullerenes C<sub>60</sub> and C<sub>70</sub> with metal-free tetraphenylporphyrin, H<sub>2</sub>TPP, as well as with manganese(II), cobalt(II), copper(II), zinc(II), and iron(III) chloride tetraphenylporphyrinates.

## Results

The new molecular complexes **1–12**, listed in Table 1, were obtained by the evaporation of solutions containing a fullerene and the corresponding porphyrin compound. The choice of the solvent is crucial. Thus, the fullerene complex of [Mn(tpp)] could be obtained only in CS<sub>2</sub>, while the complexes of H<sub>2</sub>TPP were obtained in benzene and toluene. [Cu(tpp)] and [Co(tpp)] form complexes with fullerenes in all of these solvents, while we could not isolate the complexes of [Ni(tpp)] with C<sub>60</sub> or C<sub>70</sub> at all. All complexes were isolated as well-formed crystals, but some are unstable, decaying slowly in air and even in argon through the loss of solvent. Two kinds of crystals, **1** and **2**, were obtained from C<sub>60</sub> and H<sub>2</sub>TPP; their

Table 1. Element analysis, absorption bands of solvent in the IR spectra, and the content of a solvent (according to TGA data) in **1–12**.

Complex	Elemental analysis [%]:				M	Solvent	[ $\bar{\nu}$ [cm <sup>-1</sup> ]]	[%]
	C	H	N	S				
<b>1</b>	H <sub>2</sub> TPP·2C <sub>60</sub> ·3C <sub>6</sub> H <sub>6</sub>						675, 1474, 3031	6.8
<b>2</b>	H <sub>2</sub> TPP·2C <sub>60</sub> ·4C <sub>6</sub> H <sub>6</sub>						675, 1474, 3031	11.4
<b>3</b>	H <sub>2</sub> TPP·C <sub>70</sub> ·2C <sub>6</sub> H <sub>6</sub>	92.86	2.70	3.76	–	–	675, 1474, 3031	7.8
		93.92	2.60	3.48				
<b>4</b>	[Mn(tpp)]·C <sub>70</sub> ·1.25CS <sub>2</sub>	85.14	2.14	3.68	4.86	–	1508	N/A
		86.41	1.74	3.47	4.96	3.42		
<b>5</b>	[Co(tpp)]·C <sub>60</sub> ·0.5CS <sub>2</sub>	89.41	1.89	4.03	1.61	–	1508	3.0
		87.93	1.95	3.78	2.22	4.12		
<b>6</b>	[Co(tpp)]·C <sub>70</sub>	90.15	2.12	3.76	< 0.98	–	absent	0
		90.55	1.85	3.70	0	3.90		
<b>7</b>	[Cu(tpp)]·C <sub>60</sub> ·C <sub>7</sub> H <sub>8</sub>	88.80	2.18	4.10	–	–	674, 2922 <sup>[a]</sup>	5.7
		89.61	2.30	3.78	–	4.31		
<b>8</b>	[Cu(tpp)] <sub>2</sub> ·C <sub>60</sub>						absent	0
<b>9</b>	[Cu(tpp)]·C <sub>70</sub> ·2C <sub>7</sub> H <sub>8</sub>	89.74	2.06	3.53	–	–	674, 2928 <sup>[a]</sup>	12.8
		90.30	2.24	3.48	–	3.98		
<b>10</b>	[Cu(tpp)]·C <sub>70</sub> ·1.5C <sub>7</sub> H <sub>8</sub> ·0.5C <sub>2</sub> HCl <sub>3</sub>						674, 2928 <sup>[a]</sup>	N/A
<b>11</b>	[Zn(tpp)(C <sub>5</sub> H <sub>5</sub> N)] <sub>2</sub> ·C <sub>60</sub>	84.27	2.76	6.20	0	–	702, 1440, 3080	12.0
		84.94	2.95	6.26	0	5.85		
<b>12</b>	[FeCl(tpp)] <sub>2</sub> ·C <sub>60</sub>	–	–	4.97	3.67 <sup>[b]</sup>	–	absent	0
		83.52	2.63	5.26	3.33 <sup>[b]</sup>	5.26		

[a] Toluene absorption bands at 730, 1490 and 3031 cm<sup>-1</sup> coincide with absorption bands of the donor. [b] Cl [%].

$\text{H}_2\text{TPP} \cdot 2\text{C}_{60} \cdot n\text{C}_6\text{H}_6$  stoichiometries differ only by the amount of the crystallisation solvent ( $n = 3$  or  $4$ , respectively). It is noteworthy that relative yields of **1** and **2** depend on the crystallisation temperature. Complex **1** is formed at lower temperature, it loses solvent on storage and can be preserved only under an atmosphere, saturated with benzene vapour. Complex **2**, which precipitated at higher temperature, is air-stable although it contains more solvent than **1**. This suggests that here we have kinetic (**1**) and thermodynamic (**2**) forms. Thermogravimetric data (see below) also indicates that the solvent is not strongly bound in the crystals. Notably, the mixed-solvent solvate **10** is more stable than its single-solvent analogue **9**.

In some cases, the presence of other substances was essential for crystallisation of the complexes. Hence,  $[\text{Zn}(\text{tpp})]$  forms a complex (**11**) with  $\text{C}_{60}$  only in the presence of pyridine (Py). Our preliminary single-crystal X-ray data identified **11** as a molecular complex of fullerene with the mixed-ligand porphyrinate  $[\text{Zn}(\text{tpp})(\text{Py})]$ ; the Zn atom has a tetragonal-pyramidal coordination environment. Evaporation of solution of  $[\text{Cu}(\text{tpp})]$  and  $\text{C}_{60}$  in toluene leads to the precipitation of the toluene solvate **7**, but if ferrocene is added to the solution, then, surprisingly, only the solvent-free complex **8** is precipitated. Thus, ferrocene deters the solvent from inclusion into the growing crystal, without taking its place in the structure!

The compounds were studied using thermogravimetry, and ESR, IR, UV-visible, and X-ray photoelectron spectroscopy; the crystal structures of **1**, **2**, **8** and **10** were determined by single-crystal X-ray diffraction. All the complexes are dielectrics with conductivity  $< 10^{-7} \text{ S cm}^{-1}$ .

**Thermogravimetry:** Compounds **1** and **2** begin to lose solvent at the temperatures of 150 and 120 °C, respectively, while compounds **5** and **7** do so at 170–190 °C. The first and the second toluene molecules in **9** are removed in two distinct temperature ranges, starting at 110 °C and 190 °C, respectively. The onset of the pyridine removal from **11** is much higher at 230 °C. Further loss of mass due to partial decomposition of porphyrins is observed at temperatures upward from 470 °C for  $\text{H}_2\text{TPP}$  (in complexes **1–3**), 480 °C for  $[\text{Co}(\text{tpp})]$  in **5**, 550 °C for  $[\text{Cu}(\text{tpp})]$  in **7–9** and  $[\text{Zn}(\text{tpp})]$  in **11**.

**X-ray crystal structures:** Rhombohedral complex **1** and monoclinic **2** are examples of “quasi-polymorphs”, which differ by the amount of the crystallisation solvent (see above). In both structures the fullerene molecule has no crystallographic symmetry; the  $\text{H}_2\text{TPP}$  molecule occupies an inversion centre and its chromophore moiety is sandwiched between two fullerene molecules (Figure 1). The fullerenes form the shortest contacts with the most electron-rich (nitrogen) atoms of the donor molecule. The  $\text{N} \cdots \text{C}(\text{C}_{60})$  distances of 3.02 Å in **1** and 2.96 Å in **2** lie at the lower end of the range of van der Waals contacts and well below the “standard” contact distance (3.2–3.3 Å).<sup>[21]</sup> Two of the phenyl substituents of the  $\text{H}_2\text{TPP}$  molecule form contacts with hexagonal faces of two other  $\text{C}_{60}$  molecules, with which they form dihedral angles of 21° in **1**, 13° in **2** and the shortest  $\text{C} \cdots \text{C}$  contacts of 3.41–3.52 Å in **1** and 3.36–3.70 Å in **2**. Relative disposition of the

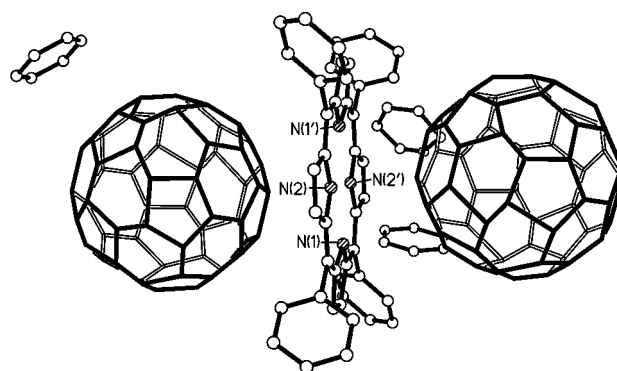


Figure 1. Molecules in the crystal of  $\text{H}_2\text{TPP} \cdot 2\text{C}_{60} \cdot 3\text{C}_6\text{H}_6$  (**1**).

two contacting  $\text{C}_6$  rings resembles the “parallel-displaced” packing of benzene rings, favourable for quadrupole–quadrupole interactions.<sup>[22]</sup>

Both structures contain three crystallographically nonequivalent molecules of solvent benzene; one of them occupies a general position and is stacked to a hexagonal face of the fullerene molecule (forming  $\text{C} \cdots \text{C}$  contacts of 3.47–3.74 Å in **1**, 3.33–3.61 Å in **2**). In **1** another benzene molecule occupies a  $\bar{3}$  special point and the third one is disordered between three positions related by a threefold symmetry axis; in **2** both remaining benzene molecules occupy inversion centres. These molecules have no close contacts with the fullerene units.

Notwithstanding these apparent similarities, the overall supramolecular organisations of **1** and **2** are drastically different. In **1** the fullerene molecules, with their six-membered rings facing one another, form a “honeycomb” motif (Figure 2) with continuous channels. Each channel runs

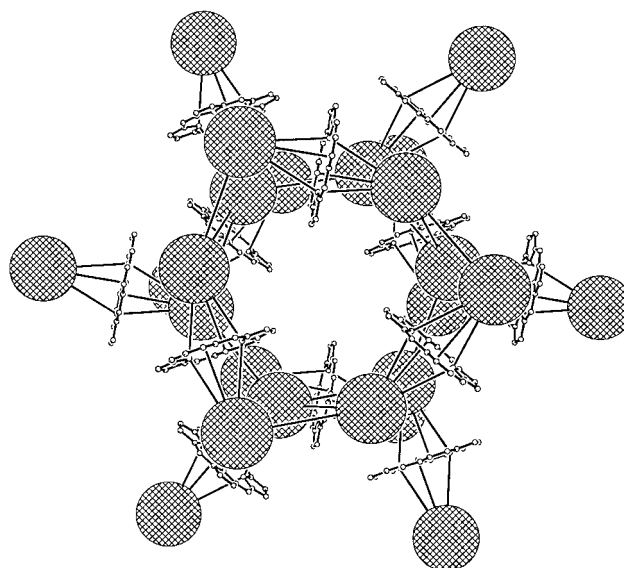


Figure 2. Crystal packing of **1**.  $\text{C}_{60}$  molecules are shown as spheres; phenyl groups and benzene molecules are omitted.

along a crystallographic threefold axis. The  $\text{H}_2\text{TPP}$  molecules have their porphyrin cores incorporated into the walls of the channels, while their phenyl groups fill the channels together with the benzene of crystallisation. Each  $\text{C}_{60}$  molecule

contacts five others with centroid...centroid separations of 9.81 Å (two), 9.85 Å (one) and 9.95 Å (two). The first three contacts are shorter than in the structure of pure  $C_{60}$  (9.94 Å at 153 K<sup>[23]</sup>) and in most of its noncovalent complexes (9.85–10.20 Å, according to the April 2000 release of the Cambridge Crystallographic Database<sup>[24]</sup>). A possible explanation of the shortening can be the induced anisotropy of the electron distribution in the fullerene, that is, polarisation effects not cancelling each other in the solid state;<sup>[5]</sup> this is more likely when fullerene packing has relatively low dimensionality (cf. in the crystal of  $C_{60}$  each molecule is surrounded by 12 others). However, the bond geometry of the cage gives no indication of such anisotropy. It is also noteworthy that another fullerene-porphyrin complex,  $[FeCl(oep)] \cdot C_{60} \cdot CHCl_3$ , also displays a short centroid...centroid distance, 9.80 Å.<sup>[16]</sup> The closest inter-fullerene C...C distances in **1**, 3.24 Å, are marginally shorter than twice the van der Waals radius of carbon (3.42 Å).<sup>[21a]</sup>

In **2** the fullerene molecules form layers of an hexagonal (graphite-like) pattern, strongly distorted by puckering; the  $H_2TPP$  molecule is sandwiched between two  $C_{60}$  molecules belonging to different layers (Figure 3). Each  $C_{60}$  molecule forms only three direct contacts to three others with centroid...centroid distances of 9.93–10.14 Å, so that a 6/6 bond of one molecule is oriented against a hexagonal face of another. Other centroid...centroid separations exceed 12 Å. This framework has channels (filled by the benzene of crystallisation) running *parallel* to the pseudo-hexagonal fullerene layers (Figure 3). The fullerene molecule is disordered between two orientations (65:35%) that are related by a 60° rotation around the molecular threefold axis. The positions of 24 carbon atoms (two opposite six-membered rings and six

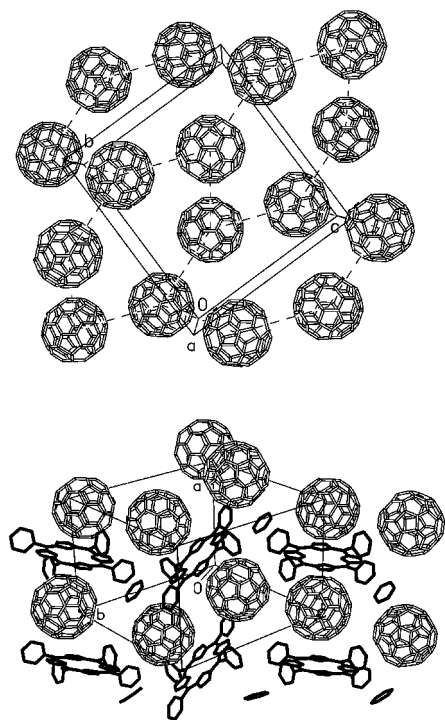


Figure 3. Crystal structure of  $H_2TPP \cdot 2C_{60} \cdot 4C_6H_6$  (**2**). Top: a layer of  $C_{60}$  molecules, parallel to the (100) plane. Bottom: a view along this layer. Only major orientations of the  $C_{60}$  molecules are shown.

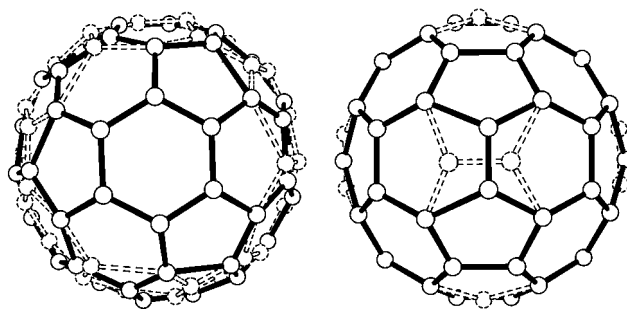


Figure 4. Rotational disorder of a  $C_{60}$  molecule (one hemisphere is shown). Left: in **2**, a 60° rotation around the threefold axis. Right: in **8**, a 180° rotation around the axis through the midpoint of 5/6 edges.

atoms directly bonded to either ring) coincide in both orientations, whereas the equatorial belt of the  $C_{60}$  cage between them is disordered (Figure 4). This type of rotational disorder was observed earlier for molecular complexes of  $C_{60}$  with dibenzotetrafulvalene<sup>[3b]</sup> and *catena*-cyclotrivertylene.<sup>[4b]</sup> The final difference Fourier map of **1** also suggests the presence of some orientational disorder that we could not rationalise entirely.

The crystal structure of **8** contains no solvent and the  $[Cu(tp)]$  molecule is located in a general position. The  $C_{60}$  molecule lies on a crystallographic twofold axis, which passes through the molecular centroid and the midpoints of two 5/6 bonds, that is, intersects the *molecular* twofold axis at a 60° angle. Thus the molecule is disordered between two orientations related by the crystallographic axis (Figure 4). This type of rotational disorder, with the disordered C–C bonds forming six crosses on the surface of a  $C_{60}$  molecule, has also been described earlier.<sup>[25]</sup> Fullerene molecules are arranged in nonlinear columns (chains), parallel to the  $z$  axis of the crystal lattice, whereby each fullerene molecule has contacts to two others with a centroid...centroid separation of 9.92 Å, which is longer than in **1** but still close to the lower limit of the usual range of such distances (see above). The resulting short inter-fullerene C...C distances (3.1–3.4 Å) involve 5/6 bonds of the contacting cages, as in  $[K([18]crown-6)]_3 \cdot C_{60} \cdot PhMe$ , in which such contact was regarded as a shift towards formation of one-dimensional polyfulleride by [2+2] cycloaddition of the 5:6 ring connections.<sup>[1c]</sup> The fullerene columns are separated from one another by pairs of warped  $[Cu(tp)]$  molecules (Figure 5). The shortest intermolecular distances  $N \cdots C(C_{60})$  of 3.36 Å and  $Cu \cdots C(\text{porphyrin})$  of 3.28 Å are

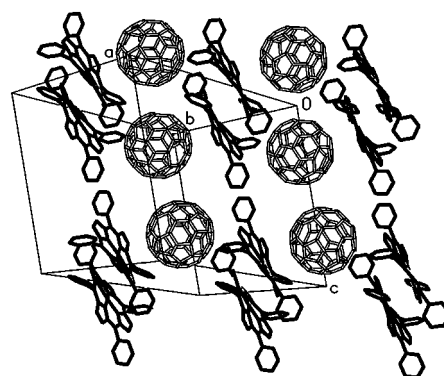


Figure 5. Molecular packing in  $[Cu(tp)]_2 \cdot C_{60}$  (**8**), projection on the plane (1–10).

characteristic of van der Waals interactions, and there are no shortened  $\text{Cu}\cdots\text{C}(\text{C}_{60})$  contacts. The packing motif is broadly similar to that of  $[\text{M}^{\text{II}}(\text{oep})]\cdot\text{C}_{60}\cdot\text{C}_6\text{H}_6\cdot\text{CHCl}_3$ ,<sup>[16]</sup> but in the latter the porphyrin chromophores remain planar and the fullerene cage is surrounded (“solvated”) by its ethyl substituents. In **8**, the  $[\text{Cu}(\text{tpp})]$  has no such flexible substituents and can maximise its van der Waals interactions with the fullerene by making the chromophore itself concave.

In the structure of **10**, the  $\text{C}_{70}$  molecule has no crystallographic symmetry and is fully ordered. Two crystallographically nonequivalent  $[\text{Cu}(\text{tpp})]$  molecules are located at inversion centres; each of their phenyl groups is disordered between two orientations with nearly equal occupancies and has no shortened contacts with the  $\text{C}_{70}$ . One independent toluene molecule occupies a general position, another one is located at an inversion centre; both molecules are disordered. The crystal contains a nonstoichiometric amount of trichloroethylene; its molecule is situated in a general position and is disordered between three orientations with the *total* occupancy of approximately 0.5. Ellipsoidal  $\text{C}_{70}$  molecules form zigzag chains parallel to the *y* axis, the same structural motif as found in  $[\text{Ni}(\text{odmap})]\cdot\text{C}_{60}$ <sup>[17]</sup> and  $\text{H}_2\text{TPP}\cdot\text{C}_{60}\cdot 3\text{PhMe}$ .<sup>[18a]</sup> Each  $\text{C}_{70}$  molecule is adjacent to two others, with close van der Waals contacts ( $\text{C}\cdots\text{C}$  3.2–3.4 Å) and centroid $\cdots$ centroid separations of 10.14 and 11.13 Å.

Each  $[\text{Cu}(\text{tpp})]$  chromophore is sandwiched between two fullerene molecules (Figure 6), whose two 6/6-type bonds “g” (adjacent to the equatorial belt of the molecule, see Scheme 1) complete the square-planar coordination of the copper atom to a distorted (tetragonally elongated) octahedral one; the  $\text{Cu}\cdots\text{C}(\text{C}_{70})$  distances varying from 2.88 to 3.03 Å. On the other hand, each  $\text{C}_{70}$  is coordinated (through the g-type bonds of the same hemisphere) with two  $[\text{Cu}(\text{tpp})]$  chromophores, whose planes form a dihedral angle of 39° between them and are nearly parallel (inclined by 7° and 10°) to the long axis of the ellipsoidal  $\text{C}_{70}$ . The same “side-on” approach of  $\text{C}_{70}$  to porphyrin was observed in  $[\text{Zn}(\text{tpp})]\cdot\text{C}_{70}$ <sup>[18a]</sup> and in the series of isostructural complexes  $[\text{M}^{\text{II}}(\text{oep})]\cdot\text{C}_{70}\cdot\text{C}_6\text{H}_6\cdot\text{CHCl}_3$  ( $\text{M}=\text{Co}, \text{Ni}$  and  $\text{Cu}$ ).<sup>[16]</sup> In the latter the long axis of the  $\text{C}_{70}$  is inclined by about 16° to the porphyrin plane. This arrangement contrasts with the “end-on” coordination of  $\text{C}_{70}$  with metals; this occurs where back-bonding is significant.<sup>[26]</sup>

The crystal lattice of **10** and the positions of the fullerene and porphyrin units therein are practically identical with

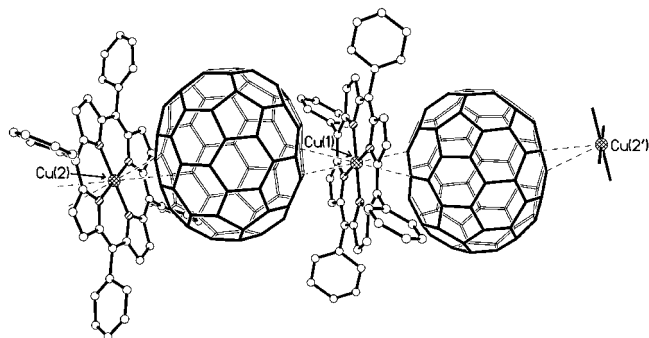
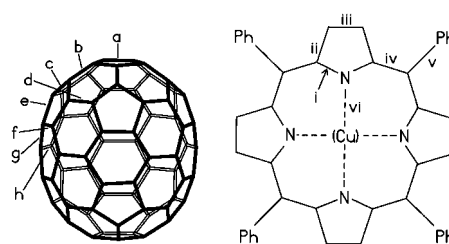


Figure 6. Chain of  $\text{C}_{70}$  and  $[\text{Cu}(\text{tpp})]$  molecules in the crystal of  $[\text{Cu}(\text{tpp})]\cdot\text{C}_{70}\cdot 1.5\text{C}_7\text{H}_8\cdot 0.5\text{C}_2\text{HCl}_3$  (**10**).



Scheme 1. Notation of chemically nonequivalent bonds in  $\text{C}_{70}$  and in  $\text{H}_2\text{TPP}$  or  $[\text{Cu}(\text{tpp})]$ .

those of  $[\text{Zn}(\text{tpp})]\cdot\text{C}_{70}$ .<sup>[18a]</sup> However, the latter structure was not reported to contain any solvent of crystallisation. Our analysis of the crystal packing in  $[\text{Zn}(\text{tpp})]\cdot\text{C}_{70}$  revealed substantial voids. Taking into account the relatively high discrepancy factor  $R=10.2\%$  and residual electron density ( $1.9\text{ e}\text{Å}^{-3}$ ), one may guess that the crystal in fact does contain some solvent (toluene?), which was not identified because of intense disorder, similar to that actually observed in **10**. The latter structure was refined to a similar  $R$  of 10.0%, but on nearly double the number of reflections.

It is also interesting to compare the structures of **10** and  $[\text{Cu}(\text{tmtaa})]\cdot\text{C}_{60}$ ,<sup>[15d]</sup> in which the metal-macrocylic system is also sandwiched between fullerene molecules, but has a rigid saddle shape that matches the fullerene curvature. This improves the overall interaction between the two, but at the same time weakens the  $\text{Cu}\cdots\text{C}_{60}$  interactions (the shortest  $\text{Cu}\cdots\text{C}$  distances are 3.18 and 3.37 Å). Fullerene molecules in  $[\text{Cu}(\text{tmtaa})]\cdot\text{C}_{60}$  form corrugated layers (as in **2**) rather than chains (as in **10**), and each  $\text{C}_{60}$  molecule has contacts to five others (as in **1**), but at longer centroid $\cdots$ centroid distances of 9.96–10.08 Å.

The  $\text{C}_{60}$  and  $\text{C}_{70}$  geometry in the complexes is in good agreement with that in pure fullerenes or their neutral molecular complexes<sup>[23, 27]</sup> (see Table 2, notation in Scheme 1). Bond lengths in the porphyrin and metal-porphyrin chromophores also remain essentially the same as in pure components and their solvates<sup>[28–32]</sup> (Table 2, Scheme 1) and fit an approximate local fourfold symmetry. However, neither is true for *conformation* of the porphyrins. Generally, a porphyrin system has two stable conformations: the planar and the warped (saddle-like); the degree of puckering may be described by the root mean square (rms) deviation ( $\Delta$ ) of the atoms from the mean plane. In the solid  $\text{H}_2\text{TPP}$ <sup>[28]</sup> or  $[\text{Cu}(\text{tpp})]$ ,<sup>[31]</sup> both chromophores are warped:  $\Delta=0.19$  and 0.21 Å, respectively. The puckering is further enhanced ( $\Delta=0.42$  Å) in the diprotonated porphyrin cation of  $\text{H}_4\text{TPP}(\text{ClO}_4)_2\cdot\text{C}_6\text{H}_6$ .<sup>[30]</sup> In contrast, both  $\text{H}_2\text{TPP}$  and  $[\text{Cu}(\text{tpp})]$  have planar conformation ( $\Delta=0.01$  Å) in 1:2 molecular complexes with *m*-xylene.<sup>[29, 31]</sup> In the complexes in which the porphyrin is sandwiched between two fullerene molecules, the chromophores are almost as planar ( $\Delta=0.053$  Å in **1**, 0.042 Å in **2**, 0.014 and 0.025 Å in two independent  $[\text{Cu}(\text{tpp})]$  molecules of **10**), whilst in the absence of such packing in **8** the  $[\text{Cu}(\text{tpp})]$  molecule remains as puckered ( $\Delta=0.263$  Å) as in solid  $[\text{Cu}(\text{tpp})]$ . The similar “warped” conformation was observed by Hochmuth et al. in the nickel porphyrinate complex with fullerene  $[\text{Ni}(\text{odmap})]\cdot$

Table 2. Average bond lengths, angles and root mean square deviations of atoms from the mean plane ( $\Delta$ ) in the porphyrin chromophore. Estimated standard deviations for the bond lengths and angles are 0.001–0.01 Å (M–N to C–C) and 0.1–1.0°, respectively, for the ordered moieties; up to 0.02 Å and 3.0° for the disordered ones.

	<b>1</b>	<b>2</b>	H <sub>2</sub> TPP <sup>[28]</sup>	H <sub>2</sub> TPP·( <i>m</i> -xylene) <sub>2</sub> <sup>[29]</sup>	H <sub>4</sub> TPP(ClO <sub>4</sub> ) <sub>2</sub> ·C <sub>6</sub> H <sub>6</sub> <sup>[30]</sup>	
$\Delta$ [Å]	0.053	0.042	0.189	0.010	0.417	
bond lengths [Å]						
i	1.378	1.376	1.350	1.377	1.390	
ii	1.439	1.443	1.438	1.443	1.431	
iii	1.353	1.358	1.361	1.354	1.365	
iv	1.405	1.405	1.403	1.391	1.414	
v	1.51	1.501	1.514	1.515	1.491	
bond angles [°]						
i–i	107.2	107.6	108.8	106.1	110.3	
i–ii	108.9	108.8	108.7	109.9	106.1	
i–iv	125.5	126.2	126.0	124.5	125.9	
ii–iii	107.4	107.4	106.9	107.0	108.7	
ii–iv	125.5	125.0	125.1	125.5	127.9	
iv–iv	126.2	125.3	125.1	126.9	123.2	
iv–v	116.9	117.3	117.4	116.5	118.4	
	<b>8</b>	<b>A</b>	<b>10</b>	<b>B</b>	[Cu(tpp)] <sup>[31]</sup>	[Cu(tpp)]·( <i>m</i> -xylene) <sub>2</sub> <sup>[32]</sup>
$\Delta$ [Å]	0.263	0.014	0.025	0.214	0.008	
bond lengths [Å]						
i	1.378	1.384	1.376	1.383	1.381	
ii	1.442	1.440	1.440	1.447	1.435	
iii	1.355	1.358	1.358	1.337	1.351	
iv	1.396	1.393	1.397	1.368	1.391	
v	1.498	1.491	1.503	1.489	1.500	
vi	1.983	2.001	2.009	1.980	1.997	
bond angles [°]						
vi–i	127.0	127.4	127.1	125.9	127.3	
i–i	105.8	105.2	105.6	107.9	105.4	
i–ii	110.0	110.4	110.4	107.9	110.2	
i–iv	125.1	125.4	125.8	126.5	125.8	
ii–iii	107.0	107.0	106.8	108.1	107.1	
ii–iv	124.6	124.2	123.8	125.3	124.0	
iv–iv	123.4	124.3	124.0	123.0	123.9	
iv–v	118.2	117.8	118.0	118.5	118.1	
	<b>1</b>	C <sub>60</sub> bond lengths [Å]		<b>8</b>	C <sub>60</sub> <sup>[a]</sup>	
		major	minor			
5/6 bond	1.47	1.47	1.50	1.45	1.46	
6/6 bond	1.35	1.36	1.32	1.40	1.40	
		C <sub>70</sub> bond lengths [Å]				
Bond	Type	Number in molecule		<b>10</b>	C <sub>70</sub> ·6S <sub>8</sub> <sup>[27b]</sup>	
a	5/6	10		1.45	1.44	
b	6/6	10		1.37	1.38	
c	5/6	20		1.46	1.46	
d	6/6	10		1.37	1.37	
e	5/6	20		1.45	1.46	
f	5/6	10		1.45	1.44	
g	6/6	20		1.40	1.40	
h	6/6	5		1.49	1.48	

[a] Gas-phase electron diffraction, ref. [27a].

C<sub>60</sub>, in which (as in **8**) only normal van der Waals contacts Ni···C<sub>60</sub> exist.<sup>[17]</sup>

**ESR spectra:** The ESR spectra of [Mn(tpp)], [Co(tpp)], [Cu(tpp)] and their complexes with C<sub>70</sub> at 77 K are shown in Figure 7. The spectra of the C<sub>60</sub> complexes with the same donors are similar. It is noteworthy that the ESR spectra of some complexes show a narrow weak signal with  $g = 2.0022$

and  $\Delta H_{pp} = 1.5$  G (300 K), which persists almost without changes down to 77 K. This signal, which was observed also in the spectra of the starting fullerenes, can be attributed to oxygen-containing impurities,<sup>[33]</sup> most probably to C<sub>120</sub>O<sup>−</sup>.<sup>[33c]</sup> Its intensity depends strongly on the conditions of preparation, purification and storage of fullerenes and the complexes.

Pure [Mn(tpp)] has a high spin state ( $S = 5/2$ ) and an anisotropic ESR spectrum ( $g_{\perp} = 5.9$ ,  $g_{\parallel} = 2.0$ ) with a hyperfine

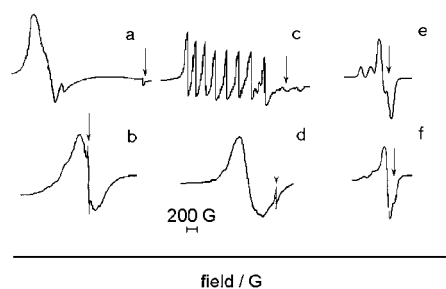


Figure 7. The ESR spectra of a) [Mn(tpp)], b) **4**, c) [Co(tpp)], d) **6**, e) [Cu(tpp)] and f) **9** at 77 K in argon atmosphere. Arrows show the position of  $g = 2.0022$ .

structure (HFS) due to the interaction between the unpaired electron and the  $^{55}\text{Mn}$  nucleus ( $I = 5/2$ ).<sup>[34]</sup> Using a solid sample with high spin concentration, we could not observe the HFS (Figure 7a). In complex **4** with  $\text{C}_{70}$ , the spin of [Mn(tpp)] is lowered to  $1/2$ . A similar spin-lowering occurs upon the formation of the nitric oxide complexes [Mn<sup>II</sup>(tpp)-(X<sup>-</sup>)(NO<sup>+</sup>)] ( $X = \text{Cl}, \text{CH}_3\text{CO}_2$ ), which show a six-line isotropic ESR spectrum with a  $^{55}\text{Mn}$  ( $I = 5/2$ ) hyperfine splitting characteristic of a low spin [ $d^5$ ] ( $S = 1/2$ ) state of [Mn<sup>II</sup>(tpp)].<sup>[34]</sup> The spectrum of **4** in argon atmosphere at 77 K (Figure 7b) is a broad line with  $g = 2.002$  and  $\Delta H_{\text{pp}} = 300$  G, but a ten-minute exposure of the sample to air reveals the HFS (six lines with the  $A_1$  intervals of 83 G). Evidently, a partial oxidation of [Mn<sup>II</sup>(tpp)] to diamagnetic [Mn<sup>III</sup>(tpp)] takes place, the concentration of spins decreases and, therefore, HFS of the unpaired electron and  $^{55}\text{Mn}$  nucleus is revealed. Incidentally, this confirms that the unpaired electron is located basically on the  $d$  orbital of Mn<sup>II</sup> and interacts with its nucleus intramolecularly. The exposure of **4** to air for a few hours results in the disappearance of the ESR signal due to complete oxidation of the paramagnetic Mn<sup>II</sup>.

The [Co(tpp)] and [Cu(tpp)] units in complexes **5–10**, as the corresponding pure porphyrins, have a low-spin state ( $S = 1/2$ ) and ESR spectra with the resolved HFS and  $g$ -factor anisotropy. The effect of the complexation is practically confined to the hyperfine interaction (HFI) parameters, which are most sensitive to local interactions on the metal centres. ESR of pure [Co(tpp)] is observed at 77 K ( $^{59}\text{Co}$ ,  $I = 7/2$ ,  $g_{\perp} = 3.322$ ,  $B = 395 \times 10^{-4} \text{ cm}^{-1}$ ,  $g_{\parallel} = 1.798$ ,  $A = 197 \times 10^{-4} \text{ cm}^{-1}$ , see Figure 7c), but not at room temperature (due to short relaxation times<sup>[35]</sup>), while the spectra of **5** and **6** (Figure 7d) are observed even at room temperature. Both complexes display a broad intense asymmetric line with  $\langle g \rangle = 2.4$  and  $\Delta H_{\text{pp}} = 500\text{--}600$  G, resulting from the overlap of parallel and perpendicular components of the spectrum of a polycrystalline sample. The HFS due to the interaction of the unpaired electron with the  $^{59}\text{Co}$  nucleus ( $I = 7/2$ ) is also observed above a broad signal, as eight components with a separation of 170 G. The  $g$  factors change substantially relative to pure [Co(tpp)], both HFI constants  $A$  and  $B$  decrease, suggesting weak [Co(tpp)] $\cdots$ fullerene interactions, probably similar for  $\text{C}_{60}$  and  $\text{C}_{70}$ .

The ESR spectra of [Cu(tpp)] in the complexes **7–10** with  $\text{C}_{60}$  and  $\text{C}_{70}$  also correspond to the low-spin state with the retention of the  $g_{\perp}$  and  $g_{\parallel}$  values. The ESR spectra of pure

[Cu(tpp)] at 77 K ( $\text{Cu}$ ,  $I = 3/2$ ,  $g_{\perp} = 2.071$ ,  $B = -29 \times 10^{-4} \text{ cm}^{-1}$ ,  $g_{\parallel} = 2.193$ ,  $A = -202 \times 10^{-4} \text{ cm}^{-1}$ )<sup>[35]</sup> and of **7** ( $g_{\perp} = 2.050$ ,  $g_{\parallel} = 2.190$ ,  $A = -168 \times 10^{-4} \text{ cm}^{-1}$ ) are even more similar. For **9** ( $g_{\perp} = 2.058$ ,  $g_{\parallel} = 2.176$ ,  $A = -170 \times 10^{-4} \text{ cm}^{-1}$ ) and **10** the values of  $g_{\perp}$  and  $g_{\parallel}$  remain almost unchanged, but the intensity of the perpendicular component increases (Figure 7f). This indicates a less anisotropic interaction of the spin orbitals, probably due to weak  $\text{Cu}\cdots$ fullerene coordination, such as we observed in the crystal structure of **10**. Earlier, changes in the ESR spectrum of the solid porphyrazine complex [Cu(odmap)]<sub>2</sub>· $\text{C}_{60}$ · $2\text{C}_6\text{H}_6$ , compared with [Cu(odmap)] in solution, were attributed<sup>[17]</sup> to similar weak  $\text{Cu}\cdots\text{C}_{60}$  interactions (as well as to stacking porphyrin $\cdots$ porphyrin interactions which do not exist in the crystal of **10**).

Pure [FeCl(tpp)] has a high-spin ( $S = 5/2$ ) state and an anisotropic ESR spectrum with  $g = 5.7$  and  $\Delta H_{\text{pp}} = 300$  G at room temperature; the signal is narrowed to 200 G on cooling down to 77 K. The spectrum of its complex **12** is almost the same, with  $g = 5.63$  and  $\Delta H_{\text{pp}} = 330$  G at room temperature and  $g = 5.78$  and  $\Delta H_{\text{pp}} = 200$  G at 77 K, indicating the absence of Fe<sup>III</sup> $\cdots\text{C}_{60}$  coordination, in agreement with the X-ray structural data.<sup>[16]</sup>

**IR spectra:** The IR spectra of all the complexes are a superposition of the vibrational bands from starting (metal)-porphyrins, fullerenes and solvents. The typical spectra of **5**, **6** and [Co(tpp)] are presented in Figure 8. The vibration

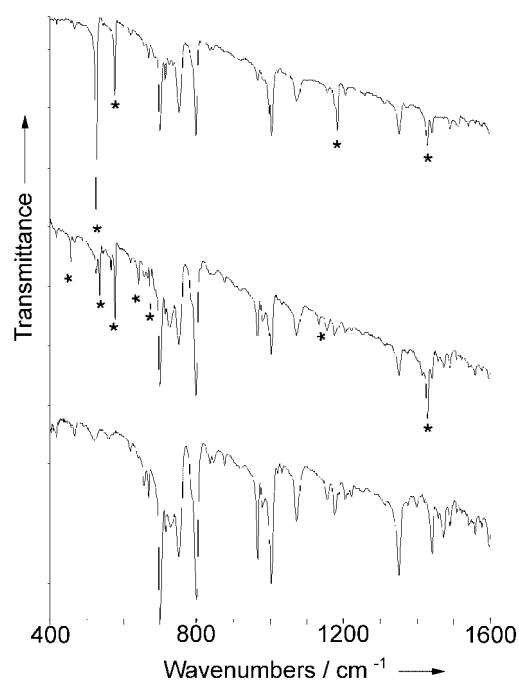


Figure 8. The IR spectra of **5** (top), **6** (middle) and [Co(tpp)] (bottom) in KBr pellets. The  $\text{C}_{60}$  and  $\text{C}_{70}$  absorption bands are marked by asterisks.

frequencies of  $\text{C}_{60}$  at  $1429 \text{ cm}^{-1}$  and  $\text{C}_{70}$  and  $1430 \text{ cm}^{-1}$ , the most sensitive to the alterations of electron density,<sup>[36]</sup> remain unchanged within  $\pm 1 \text{ cm}^{-1}$ , indicating the absence of a charge transfer in the ground state. The porphyrin bands in the

complexes also coincide with those of the pure porphyrins. Larger shifts (up to  $5\text{ cm}^{-1}$ ) upon the complex formation were observed for C–C ( $700\text{--}800\text{ cm}^{-1}$ ) and C–H vibrations ( $3000\text{--}3100\text{ cm}^{-1}$ ) of phenyl groups and N–H vibrations of  $\text{H}_2\text{TPP}$  at  $3320\text{ cm}^{-1}$ .

**UV-visible spectra:** Van der Waals interactions of porphyrins with fullerenes failed to generate additional bands in the UV-visible spectra of any of the studied complexes except **4**, which shows an intense absorption band at  $487\text{ nm}$  (Figure 9) that is

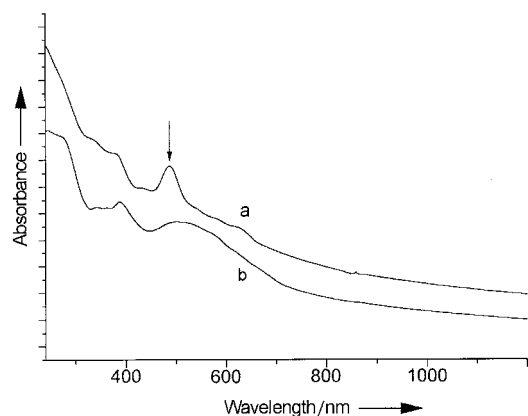


Figure 9. The UV-visible spectra of a) **4** and b)  $\text{C}_{70}$  in KBr matrix. The  $[\text{Mn}(\text{tpp})]$  absorption band is marked by an arrow.

not present in the spectrum of pure  $[\text{Mn}(\text{tpp})]$ . This band may correspond to the  $d\text{--}d$  transition for  $\text{Mn}^{\text{II}}$ , which is forbidden in the high-spin state of the free  $[\text{Mn}(\text{tpp})]$ , but becomes allowed as the spin lowers to  $1/2$  in the complex. Similar spin-lowering in  $[\text{Mn}^{\text{II}}(\text{tpp})(\text{CN}^-)(\text{NO}^+)]$  (see above) is also accompanied by the appearance of a new intense band at  $490\text{ nm}$  (toluene glass,  $77\text{ K}$ ).<sup>[34]</sup>

The UV-visible reflectance spectra from single crystals of **5** were measured in three different polarisations of light (parallel to the crystal faces) and the absorption spectra were derived therefrom by the Kramers–Kronig transformation. A comparison (Figure 10) with the absorption spectrum of

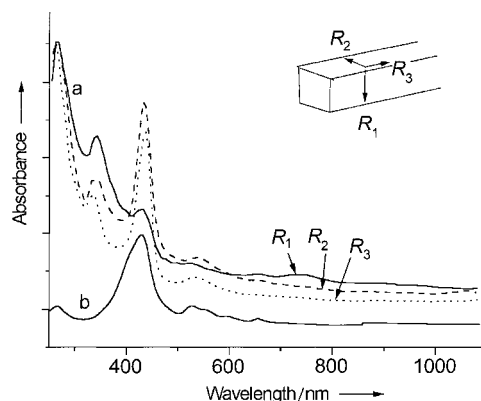


Figure 10. The UV-visible absorption spectra: a) of a single crystal of **5** for three polarisations of light  $R_{1-3}$  (parallel to the crystal faces); b) of  $[\text{Co}(\text{tpp})]$  in a KBr pellet.

$[\text{Co}(\text{tpp})]$  (in KBr pellet) shows that the spectrum of **5** ( $263$ ,  $340$ ,  $433$  and  $533\text{ nm}$ ) is a superposition of the slightly shifted bands of  $[\text{Co}(\text{tpp})]$  ( $429$  and  $527\text{ nm}$ ) and  $\text{C}_{60}$  ( $262$  and  $340\text{ nm}$ ). However, the absorption bands of  $[\text{Co}(\text{tpp})]$  in **5** are anisotropic and have the maximum intensity in the  $R_2$  and  $R_3$  polarisations, suggesting that the planes of the porphyrin chromophores are almost parallel to the  $R_2$  and  $R_3$  directions of the crystal. The intensity of a broad weak band near  $750\text{ nm}$  in the  $R_3$  polarisation is dependent on the polarisation and can be attributed to a  $[\text{Co}(\text{tpp})] \rightarrow \text{C}_{60}$  charge transfer (CT) in the direction normal to the porphyrin plane. The spectra of other complexes (Table 3) contain no pronounced CT bands, while

Table 3. UV-visible spectra.

	Absorption bands [nm]	
	fullerene	porphyrin
$\text{C}_{60}$	260, 340	–
$\text{C}_{70}$	344, 388, 501	–
$\text{H}_2\text{TPP}$	–	432, 523
<b>1</b>	261, 336	438, 523
$[\text{Mn}(\text{tpp})]$	–	426, 580, 620
<b>4</b>	337, 387	487, 620
$[\text{Co}(\text{tpp})]$	–	429, 527
<b>5</b>	263, 340	433, 533
<b>6</b>	256, 337	431, 526
$[\text{Cu}(\text{tpp})]$	–	427, 547
<b>9</b>	263, 339	432, 551

showing bathochromic shifts (up to  $6\text{ nm}$ ) of the Soret and Q bands of the porphyrin units compared to pure porphyrins. Similar effects *in solution* were observed earlier for cyclophane-type dyad compounds,<sup>[10b]</sup> in which a  $\text{C}_{60}$  fullerene and an  $\text{H}_2\text{-}$  or zinc(II) diphenylporphyrin moieties are linked by covalent bridges and, therefore, are constrained to a face-to-face contact at  $3.9\text{--}4.1\text{ \AA}$ . There too, the UV spectrum was the superposition of the components' spectra, in the visible region the Soret bands underwent a bathochromic shift and a strong intensity decrease, whereas the Q bands were less affected. The latter was taken as an indication that the electronic structure of the porphyrin is strongly perturbed by the fullerene, but not vice versa.

**X-ray photoelectron spectra:** The  $\text{N}1s$ ,  $\text{Co}2p_{3/2}$  and  $\text{Cu}2p_{3/2}$  peaks of the donor units in the complexes (Table 4) are only slightly shifted relative to the starting porphyrins, indicating

Table 4. X-ray photoelectron spectra.

	$\Delta\text{C}1s$ [eV] <sup>[a]</sup>	$\text{N}1s$ [eV] <sup>[b]</sup>	$\text{M}2p_{3/2}$ [eV] <sup>[b]</sup>
$\text{C}_{60}$	1.9	–	–
$\text{H}_2\text{TPP}$	2.70	400.0, 398.2	–
<b>2</b>	2.05	399.9, 398.2	–
$[\text{Co}(\text{tpp})]$	2.30	399.0	780.6
<b>5</b>	2.05	398.8	780.3
$[\text{Cu}(\text{tpp})]$	2.20	398.2	934.6
<b>7</b>	2.20	399.0	934.6
<b>9</b>	2.10	398.7	934.2

[a] Halfwidth of the  $\text{C}1s$  peak. [b] Peak positions ( $\pm 0.2\text{ e}$ ),  $\text{M} = \text{Co}$  or  $\text{Cu}$ .

no significant redistribution of electron density. The C1s peak halfwidth of **2** is narrower than that of pure H<sub>2</sub>TPP (Figure 11), and both display satellite structures at higher energies relatively to the basic C1s. This satellite structure is narrower for H<sub>2</sub>TPP than for **2**, probably because of their different

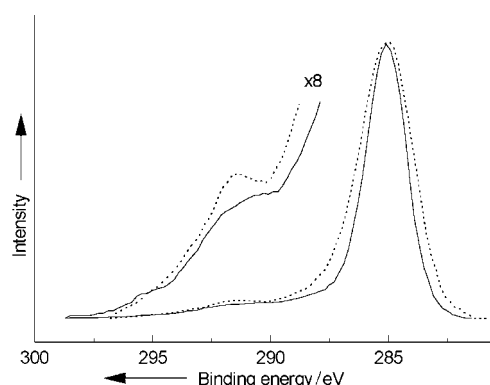


Figure 11. X-ray photoelectron C1s spectra of H<sub>2</sub>TPP (dashed) and **2** (solid line), and a portion thereof multiplied eight times.

nature: the former originates from the  $\pi-\pi^*$  transition in phenyl groups, the latter mainly from the losses associated with the excitation of  $\pi$  plasmons of the C<sub>60</sub>.<sup>[37]</sup> The halfwidth of the C1s peaks for [M<sup>II</sup>(tpp)] in fullerene complexes is also smaller than for the pure donors (see Table 4), while the relative integral intensity and the halfwidth of the satellite peak are larger in the former.

## Discussion

On the strength of IR, ESR, UV-visible and X-ray photoelectron spectroscopy, conductivity and crystallographic data, compounds **1–12** are essentially molecular complexes without any notable charge transfer. This could be predicted for **1–3** and **5–10**, since the oxidation potentials of H<sub>2</sub>TPP, [Cu(tpp)] (both +1.00 V) and [Co(tpp)] (+0.54 V) (in benzonitrile, vs SCE<sup>[38]</sup>) are very positive compared to the reduction potentials of C<sub>60</sub> and C<sub>70</sub>, –0.44 and –0.41 V, respectively (in dichloromethane, vs SCE<sup>[39]</sup>). However,  $E_{\text{ox}}$  of [Mn(tpp)] (–0.23 V, acetonitrile, vs SCE<sup>[40]</sup>) seems close enough to the  $E_{\text{red}}$  of C<sub>70</sub> to expect a significant CT in **4**, which does not occur. One possible explanation is that nonpolar solvents were used. Previously it was shown<sup>[12, 13]</sup> that even such strong donors as [Cr(tpp)] and [Sn(ttp)] can not reduce C<sub>60</sub> to a radical anion in nonpolar solvents, notwithstanding much more negative redox potentials ( $E_{\text{ox}} = -0.86$  and  $-1.17$  V, respectively). The formation of radical-anion salts was observed in polar media like tetrahydrofuran or *N*-methylimidazole, which stabilises [Cr(tpp)]<sup>+</sup> and [Sn(ttp)]<sup>2+</sup> cations. Unfortunately, we were unable to prepare complexes of [Mn(tpp)] with fullerenes in the CS<sub>2</sub>/THF mixture (1:1) to corroborate this hypothesis. In the case of [Co(tpp)] and C<sub>60</sub>, only a THF solvate of [Co(tpp)] without C<sub>60</sub> was obtained.

The other reason for a low extent of charge transfer in the complexes may be the low efficiency of HOMO–LUMO overlapping between porphyrin and fullerene moieties. The

absence of charge transfer from [Mn(tpp)] to C<sub>70</sub> in **4** and low-spin state of [Mn(tpp)] therein, frustrate the hope to obtain a molecular ferromagnet similar to the [Mn(tpp)][TCNE]·2PhMe salt, in which a one-dimensional ferromagnetic ordering was associated with the presence of the tetracyanoethylene (TCNE<sup>•-</sup>) radical anion and the high-spin [Mn<sup>III</sup>(tpp)]<sup>+</sup>.<sup>[13]</sup>

On the other hand, the complexes described herein can not be regarded as random combinations of essentially inert components. Rather they belong to the (yet insufficiently understood) class of molecular complexes in which a cumulative effect of weak  $\pi-\pi$ , electrostatic (multipole) and dispersion forces results in a substantial mutual affinity of the components without any appreciable charge transfer or alteration of the covalent bond geometry; C<sub>6</sub>H<sub>6</sub>·C<sub>6</sub>F<sub>6</sub> can be regarded as a typical complex of this class.<sup>[22]</sup> An indication of such affinity is the persistence of a few types of supramolecular organisation (synthons) in a variety of complexes. Thus, a zig-zag chain of fullerene cages interleaved with planar porphyrins can be discerned in every 1:1 fullerene-porphyrin complex previously reported.<sup>[17, 18]</sup> Complices with a 1:2 ratio display the same motif with each porphyrin molecule replaced by two (also planar), stacked face-to-face.<sup>[16]</sup> The former motif exists in **2** and **10** (and in a cyclic variety, in **1**); the latter in **8**, except that there the porphyrins are warped. In every case, fullerene is aligned against the centre of the porphyrin chromophore, whether the latter is occupied by a metal atom or not. 1:1 complexes of C<sub>60</sub> or C<sub>70</sub> with rigidly warped TMTAA or OMTAA systems, also comprise mixed column. Likewise, both synthons of fullerene-fullerene type, namely, a zig-zag chain of closely contacting fullerene cages and a corrugated layer thereof, which are observed in fullerene-porphyrin complexes, also exist, for example, in [Ni(tmtaa)]·C<sub>60</sub> and [Ni(omtaa)]·C<sub>60</sub>·2CS<sub>2</sub>, respectively.<sup>[15b]</sup>

This view is further corroborated by our spectroscopic and ESR studies; these indicate small but significant effects that can be attributed to the mutual influences of the fullerene and porphyrin  $\pi$  systems and correlate with the crystallographic data. Thus, N(porphyrin)···C(fullerene) contacts marginally shorter than the sum of the van der Waals radii, such as observed in **1** and **2**, are a general feature of fullerene complexes with metal-free porphyrins and were explained<sup>[18]</sup> by a favourable van der Waals attraction between curved and planar  $\pi$ -surfaces. Changing of the porphyrin conformation from warped to planar on complexation is also noteworthy. Of course, a molecule that is nonplanar in the gas phase can adopt a flat conformation in a crystal in order to maximise the packing density. However, here the nonplanar conformation is displayed in *crystals* of pure porphyrins and, furthermore, planarisation of the porphyrin chromophore is unlikely to facilitate its co-crystallisation with a *spherical* fullerene molecule. In fact, conformationally flexible molecules often adopt folded conformations to “wrap” around a fullerene cage, for example, a tetrathiafulvalene derivative in DBTTF·C<sub>60</sub>·C<sub>6</sub>H<sub>6</sub>.<sup>[3b]</sup> Therefore the porphyrin planarisation may be due to intermolecular interactions rather than packing requirements. Rigid saddle-shaped macrocyclic complexes [M<sup>II</sup>(tmtaa)] and [M<sup>II</sup>(omtaa)] can accommodate a fullerene

molecule in their concave surface and achieve a better match of curvature without any change in the macrocycle shape.<sup>[15]</sup> A larger area of a host–guest contact evidently maximises the total van der Waals interaction. However, these macrocycles (and the warped porphyrin in **8**) do not form such short contacts with fullerenes, as the planar porphyrins do. Also, as could be expected, maximisation of the fullerene–macrocycle interaction diminishes the fullerene–fullerene interactions. In “disparate” fullerene-porphyrin complexes, distances between the centroids of  $C_{60}$  molecules are often shorter than the doubled van der Waals radius of 5.0 Å,<sup>[41]</sup> especially in **1** and  $[FeCl(oep)] \cdot C_{60} \cdot CHCl_3$  (see above). In the better matched fullerene–“saddle” complexes,  $C_{60}$  molecules lie further apart, or are completely insulated from direct contacts.

The contacts of a copper atom with two electron-rich fullerene 6/6 bonds in **10** is of particular interest. A distorted octahedral coordination with four strong bonds and two weak ones (*trans* to each other) is very common for  $Cu^{II}$  due to the Jahn–Teller effect. A survey of the October 1999 release of the Cambridge Structural Database<sup>[24]</sup> shows that the  $Cu \cdots C$  (olefin) distances are distributed in two distinct ranges, namely 1.9–2.1 Å (strong  $\eta^2$  coordination) and 3.1–3.3 Å (nonbonded contacts), with a few exceptional distances of 2.9–3.0 Å, that is, slightly shorter than van der Waals contacts (Figure 12). The  $Cu \cdots C(C_{70})$  distances in **10** (2.88–3.03 Å)

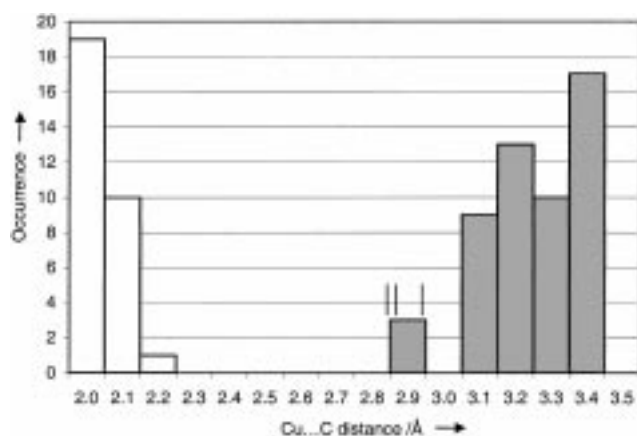


Figure 12. Histogram of bonding (white columns) and nonvalent (grey)  $Cu \cdots C$  (olefin) distances from CSD data. Secondary bonding distances in **10** are shown as thin lines.

belong to the latter category and can be described as an additional coordination (secondary bonding), which is fairly common for  $d$  elements and was reported earlier for a variety of fullerene complexes. Similar interactions of a metal atom with 6/6 bonds of  $C_{60}$  ( $M \cdots C$  2.67–3.32 Å) were observed in two isomorphous complexes  $[M^{II}(oep)] \cdot C_{60} \cdot CHCl_3$  ( $M = Co$  and  $Zn$ ).<sup>[18]</sup> In a series of isomorphous compounds  $[M^{II}(oep)] \cdot C_{70} \cdot C_6H_6 \cdot CHCl_3$  ( $M = Co, Ni$  and  $Cu$ )<sup>[18]</sup> the metal atom has an additional coordination with only one carbon atom of the  $C_{70}$  cage; the  $Cu \cdots C$  distance of 2.92 Å (cf.  $Co \cdots C$  2.80 Å and  $Ni \cdots C$  2.83 Å) is close to those in **10**. Metal  $\cdots$  fullerene interactions of the same order were also found recently in  $[Zn(tpp)] \cdot C_{70}$  (2.89 Å),<sup>[20a]</sup>  $[Fe(tpp)]B(C_6F_6)_4 \cdot C_{60}$  (2.63 Å)<sup>[20b]</sup>

and  $[Ni(odmap)] \cdot C_{60}$ .<sup>[19]</sup> As the  $C_{70}$  molecule is disordered in **8** and ordered in **10** (and also in all three  $[M^{II}(oep)] \cdot C_{70} \cdot C_6H_6 \cdot CHCl_3$  complexes), one can suggest that the additional metal  $\cdots$  fullerene coordination may be responsible for the  $C_{70}$  ordering. However, in the structure of  $[Zn(tpp)] \cdot C_{70}$  the  $C_{70}$  is also disordered.

Metal(II) tetraphenylporphyrins form complexes with  $C_{70}$  more readily than with  $C_{60}$  (e.g., **9** precipitates even from dilute solutions), while the opposite is true for substituted tetrathiafulvalenes and aromatic hydrocarbons.<sup>[11]</sup> The reasons of this may be better steric compatibility between  $[M^{II}(tpp)]$  and  $C_{70}$ . Thus,  $[Ni(omtaa)]$  can accommodate  $C_{70}$  in the same way as smaller  $[Ni(omaa)]$  accommodates  $C_{60}$ .<sup>[15d]</sup> Another reason may be the higher propensity of  $C_{70}$  for  $d-\pi$  metal–fullerene interactions: although the  $Cu \cdots C_{70}$  interactions in **10** are rather weak, they compare favourably with the absence of any such interactions in the  $C_{60}$  complex **8**. Whatever the origin of the effect, it may be utilised to separate chromatographically  $C_{60}$  from  $C_{70}$  by using appended metal tetraphenylporphyrins.

## Conclusion

New molecular complexes of fullerenes  $C_{60}$  and  $C_{70}$  with tetraphenylporphyrin, metal(II) tetraphenylporphyrins and iron(III) tetraphenylporphyrin chloride were obtained and characterised by IR, UV-visible, ESR, and XPS data. All the complexes obtained are molecular ones without charge transfer in the ground state. Single-crystal structures of four molecular complexes showed different packing of fullerene molecules varying from columnar to three-dimensional ones. In all compounds the interaction between the components is mainly of van der Waals nature, with probable contribution of  $C_{60} \cdots N(H_2TPP) \pi-\pi$  interactions and secondary  $d-\pi$  coordination  $[M(tpp)] \cdots C_{70}$ ; this last coordination mode slightly affects the electronic state of  $[M(tpp)]$ . Indirect evidence for a specific  $[M(tpp)]$ –fullerene interaction was provided by ESR spectroscopy: the effect of complexation with fullerenes on the ESR spectra of metal tetraphenylporphyrins decreases in the succession  $[Mn(tpp)] > [Co(tpp)] > [Cu(tpp)]$ , becoming negligible for  $[FeCl(tpp)]$ .

The difference in nonbonding interactions of  $[Cu(tpp)]$  with  $C_{60}$  and  $C_{70}$  observed in the complexes may be useful for chromatographic separation of these fullerenes.

According to the UV-visible spectra, the charge transfer can probably take place in the photoexcited state of the complexes, affecting the whole set of electric and magnetic properties of the complexes formed. Studies of photoinduced electron transfer in the solid state of the complexes, which are of particular interest for their optical properties, are presently under way.

## Experimental Section

**Materials:**  $[Mn(tpp)]$  was synthesised from  $H_2TPP$  and  $MnCl_2 \cdot 4H_2O$  and purified as described earlier, its elemental analysis, ESR and IR spectra coincide with the reported data.<sup>[42]</sup>  $H_2TPP$ ,  $[Co(tpp)]$ ,  $[Cu(tpp)]$ ,  $[Zn(tpp)]$

and [FeCl(tp)] were purchased from Aldrich. Fullerenes  $C_{60}$  of 99.9% purity and  $C_{70}$  of 98% purity were used. Benzene and toluene were distilled over Na/benzophenone under argon; trichloroethylene and  $CS_2$  were distilled over  $P_2O_5$  under argon. The solvents were stored under argon.

**General:** Single-crystal IR spectra were measured on a Perkin Elmer 1725X spectrophotometer, equipped with an IR microscope, in the 650–3200  $cm^{-1}$  range. The powdered samples were pressed in KBr pellets (1:400); their spectra were recorded in the 400–7000  $cm^{-1}$  range. Electronic absorption spectra were measured with a Perkin Elmer Lambda 19 UV-visible-NIR spectrophotometer in the 220–3000 nm range (KBr pellet, 1:2000). Electronic reflectance spectra of the single crystals were recorded with a microspectroreflectometer equipped with an UV-visible microscope in the 240–1150 nm range. The spectra were recorded in polarised light at room temperature. The absorption spectra were derived from the reflectance spectra by the Kramers–Kronig transformation. Thermogravimetric analysis was carried out on a Q-1000 derivatograph in quartz bowls in the argon flow at the 10–20  $K min^{-1}$  rate of heating in the 298–1273 K range. The mass-loss temperature was determined from the minimum of DTG curve. X-ray photoelectron spectra (XPS) were measured with a VIEE-15 spectrometer upon excitation by  $Mg_{K\alpha}$  radiation ( $E = 1253.6$  eV) and calibrated to the C1s peak (285.0 eV). ESR spectra were registered with a Radiopan SE/X 2547 spectrometer. The conductivity was measured by two-contact method on pressed pellets.

**Synthesis:** All complexes were obtained by the evaporation of equimolar solutions of  $C_{60}$  and corresponding porphyrin under argon during 5–10 days. The analyses of the obtained complexes are summarised in Table 1.

**$H_2TPP \cdot 2C_{60} \cdot 3C_6H_6$  (1) and  $H_2TPP \cdot 2C_{60} \cdot 4C_6H_6$  (2):** Compounds **1** and **2** were obtained by crystallisation from the same benzene solution (at room temperature) as hexagonal needles and nonrectangular prisms, respectively. The crystals were washed with acetone until the disappearance of the  $H_2TPP$  colour and dried in air. The relative yields **1** and **2** depend on the evaporation temperature; **1** is predominantly formed below 15 °C and **2** above 24 °C. The crystals of **1** slowly deteriorate on storage in air or in argon due to the loss of the solvent.

**$H_2TPP \cdot C_{70} \cdot 2C_6H_6$  (3):** Compound **3** precipitated from the benzene solution (at room temperature) as plates with quantitative yield. The crystals were washed with acetone and dried in air. They degrade on storage after several days.

**[Cu(tp)] $\cdot C_{60} \cdot C_7H_8$  (7):** Plate-like crystals of **7** were obtained from toluene in a quantitative yield. The crystals were washed with acetone and dried in air. They degrade on storage after several days.

**[Cu(tp)] $_2 \cdot C_{60}$  (8):** Compound was obtained from a solution of  $C_{60}$ , CuTPP and ferrocene (1:1:10 molar ratio) in toluene as nonrectangular prismatic

crystals in a quantitative yield. The solvent was decanted from the crystals before the precipitation of ferrocene, and the crystals were washed with acetone.

**[Cu(tp)] $\cdot C_{70} \cdot 2C_7H_8$  (9):** Compound **9** precipitated from toluene solution as prisms with a quantitative yield. The crystals were washed with acetone and dried in air. They degrade on storage after several days.

**[Mn(tp)] $\cdot C_{70} \cdot 1.25CS_2$  (4), [Co(tp)] $\cdot C_{60} \cdot 0.5CS_2$  (5) and [Co(tp)] $\cdot C_{70}$  (6):** Compounds **4–6** were obtained from  $CS_2$  as elongated parallelepipedal crystals, washed with diethyl ether until complete decoloration of the solution and dried under argon; yields 50–80% (on fullerene). Black plate-like crystals of a  $C_{60} \cdot C_{70} \cdot xCS_2$  solvate were obtained as a by-product and separated manually from the crystals of the molecular complexes under a microscope. The crystals of **4** are air sensitive and were handled in argon atmosphere.

**[Cu(tp)] $\cdot C_{70} \cdot 1.5C_7H_8 \cdot 0.5C_2HCl_3$  (10), [Zn(tp)]( $C_5H_5N$ ) $_2 \cdot C_{60}$  (11) and [FeCl(tp)] $_2 \cdot C_{60}$  (12):** Compounds **10** and **11** were obtained from trichloroethylene, with the addition of several drops of toluene and pyridine, respectively. Without these additional solvents, crystallisation does not occur. Compound **12** was crystallised from pure trichloroethylene. The crystals of parallelepipedal habit were washed with acetone and dried in air; yield 90%.

A peculiar blue lustre is characteristic for all the complexes.

**Crystal structure determination:** X-ray diffraction experiments for **1**, **2**, **8** and **10** were carried out on SMART 3-circle diffractometers with 1 K CCD area detectors in the Chemistry Department, University of Durham (**1**, **2**) and in the Centre for X-ray Structural Studies, Institute of Organometallic Compounds R.A.S. (**8**, **10**), by using graphite-monochromated  $Mo_{K\alpha}$  radiation ( $\lambda = 0.71073$  Å). The data collection nominally covered over a half (for **1**, **2**, **8**) or  $\frac{3}{4}$  (for **10**) of the reciprocal space, by a combination of four sets of  $\omega$  scans, each set with different  $\phi$  and/or  $2\theta$  angles. The absence of the crystal decay was monitored by repeating the first 50 scans at the end of the data collection and comparing the duplicate reflections. Reflection intensities were integrated using SAINT program.<sup>[43]</sup> The solution and refinement of all structures were performed with SHELXTL program package.<sup>[44]</sup> The intensity statistics were biased owing to strong anisotropic extinction that hindered the routine crystal structure determination by direct methods. The structures of **1**, **2**, and **10** were solved after omitting a group of reflections with the greatest normalized structure amplitudes in the primary set, and **8** after lowering the symmetry from the space group  $C2/c$  (later confirmed by the successful refinement) to  $C2$ . After this, all non-hydrogen atoms except some disordered ones of the fullerene skeleton or the solvent molecules, were revealed from  $E$ -syntheses, and the remaining atoms were located from the subsequent Fourier maps. The structures were refined by full-matrix least-squares against  $F^2$  of all data.

Table 5. Crystal data of **1**, **2**, **8** and **10**.

	<b>1</b>	<b>2</b>	<b>8</b>	<b>10</b>
formula	$H_2TPP \cdot 2C_{60} \cdot 3C_6H_6$	$H_2TPP \cdot 2C_{60} \cdot 4C_6H_6$	$[Cu(tp)]_2 \cdot C_{60}$	$[Cu(tp)] \cdot C_{70} \cdot 1.5C_7H_8 \cdot 0.5C_2HCl_3$
$M_r$ [g mol $^{-1}$ ]	2290.12	2368.02	2073.16	1582.67
crystal system	rhombohedral	monoclinic	monoclinic	triclinic
space group	R (No. 148)	$P2_1/c$ (No. 14)	$C2/c$ (No.15)	$P\bar{1}$ (No. 2)
$a$ [Å]	19.9967(8)	13.7422(6)	22.6284(7)	14.3756(6)
$b$ [Å]	19.9967(8)	20.765(1)	20.5604(7)	16.5497(8)
$c$ [Å]	19.9967(8)	18.626(1)	19.6828(6)	17.659(9)
$\alpha$ [°]	99.311(2)	90	90	72.460(1)
$\beta$ [°]	99.311(2)	91.814(4)	106.145(1)	86.278(1)
$\gamma$ [°]	99.311(2)	90	90	80.577(1)
$V$ [Å $^3$ ]	7640	5312	8796	3951
$Z$	3	2	4	2
$\rho_{calcd}$ [g cm $^{-3}$ ]	1.493	1.481	1.565	1.305
$\mu$ [mm $^{-1}$ ]	0.09	0.09	0.56	0.37
$T$ [K]	120	120	110	110
Max. $2\theta$ [°]	52.7	60.8	60.1	60.1
reflections measured	51 574	66 978	40 445	43 877
unique reflections	10 400	14 719	12 881	22 654
observed reflections [ $I > 2\sigma(I)$ ]	5579	10 488	8739	14 023
parameters	839	1191	706	1174
$R$ [ $I > 2\sigma(I)$ ]	0.119	0.062	0.058	0.100
$wR_2$	0.366	0.147	0.165	0.331

The ordered non-hydrogen atoms were refined in anisotropic approximation, the disordered ones in isotropic approximation, with hydrogen atoms (partially revealed in difference Fourier maps) "riding" in idealised positions. Crystal data and experimental parameters are listed in Table 5. Crystallographic data (excluding structure factors) for the structures reported in this paper have been deposited with the Cambridge Crystallographic Data Centre as supplementary publication no. CCDC-143510 (10), 143511 (8), 143512 (2) and 143513 (1). Copies of the data can be obtained free of charge on application to CCDC, 12 Union Road, Cambridge CB21EZ, UK (fax: (+44) 1223-336-033; e-mail: deposit@ccdc.cam.ac.uk).

### Acknowledgements

The work was supported by the Russian Program "Fullerenes and Atomic Clusters" and by Russian Foundation for Basic Research, grants Nos. 99-03-32810 and 00-03-32577a. A support from the University of Durham (ISN, July–October 1998) and the EPSRC funding of the Senior Research Fellowship (J.A.K.H.) are gratefully acknowledged. The authors (I.S.N. and Y.L.S.) are indebted to Prof. Mikhail Yu. Antipin for an access to the equipment and the software of the Centre for X-ray studies, Institute of Organoelement Compounds R.A.S.

- [1] a) M. J. Rosseinsky, *J. Mater. Chem.* **1995**, *5*, 1497; b) P. W. Stephens, D. Cox, J. W. Lauher, L. Mihaly, J. B. Wiley, P.-M. Allemand, A. Hirsch, K. Holzer, Q. Li, J. D. Thompson, F. Wudl, *Nature* **1992**, *355*, 331; c) T. F. Fässler, R. Hoffmann, S. Hoffmann, M. Würle, *Angew. Chem.* **2000**, *112*, 2170; *Angew. Chem. Int. Ed.* **2000**, *39*, 2091.
- [2] N. S. Sariciftci, A. J. Heeger, in *Handbook of Organic Conductive Molecules and Polymers* (Ed.: H. S. Nalwa), Wiley, **1997**, *1*, 414.
- [3] a) A. Izuoka, T. Tachikawa, T. Sugawara, Y. Suzuki, M. Konno, Y. Saito, H. Shinohara, *J. Chem. Soc. Chem. Commun.* **1992**, 1472; b) D. V. Konarev, Y. V. Zubavichus, Yu. L. Slovokhotov, Yu. M. Shul'ga, V. N. Semkin, N. V. Drichko, R. N. Lyubovskaya, *Synth. Met.* **1998**, *92*, 1.
- [4] a) M. J. Hardie, C. L. Raston, *Chem. Commun.* **1999**, 1153; b) J. L. Atwood, M. J. Barnes, M. G. Gardiner, C. L. Raston, *Chem. Commun.* **1996**, 1449.
- [5] L. J. Barbour, G. W. Orr, J. L. Atwood, *Chem. Commun.* **1997**, 1439.
- [6] D. V. Konarev, E. F. Valeev, Yu. L. Slovokhotov, Yu. M. Shul'ga, R. N. Lyubovskaya, *J. Chem. Res. (S)* **1997**, 442.
- [7] D. M. Eichhorn, S. Yang, W. Jarrell, T. F. Baumann, L. S. Beall, A. J. P. White, D. J. Williams, A. G. M. Barrett, B. M. Hoffman, *Chem. Commun.* **1995**, 1703.
- [8] a) D. V. Konarev, R. N. Lyubovskaya, *Russ. Chem. Rev.* **1999**, *68*, 19; b) D. V. Konarev, V. N. Semkin, A. Graja, R. N. Lyubovskaya, *J. Mol. Struct.* **1998**, *450*, 11.
- [9] a) J. Fujisawa, Y. Ohba, S. Yamauchi, *Chem. Phys. Lett.* **1998**, *294*, 248; b) P. M. Martino, H. W. Van, *Proc. Electrochem. Soc.* **1998**, *98*–8, 338.
- [10] a) D. Kuciauskas, S. Lin, G. R. Seely, A. L. Moore, T. A. Moore, D. Gust, T. Drovetskaya, C. A. Reed, P. D. W. Boyd, *J. Phys. Chem.* **1996**, *100*, 15926; b) N. Armaroli, G. Marconi, L. Echegoyen, J.-P. Bourgeois, F. Diederich, *Chem. Eur. J.* **2000**, *6*, 1629.
- [11] A. Penicaud, J. Hsu, C. A. Reed, A. Koch, K. Khemani, P. M. Allemand, F. Wudl, *J. Am. Chem. Soc.* **1991**, *113*, 6698.
- [12] J. Stinchcombe, A. Penicaud, P. Bhyrappa, P. D. W. Boyd, C. A. Reed, *J. Am. Chem. Soc.* **1993**, *115*, 5212.
- [13] J. S. Miller, A. J. Epstein, *Chem. Commun.* **1998**, 1319.
- [14] L. L. Gumanov, B. L. Korsounskii, *Mendeleev Commun.* **1997**, 158.
- [15] a) P. C. Andrews, J. L. Atwood, L. J. Barbour, P. J. Nichols, C. L. Raston, *Chem. Eur. J.* **1998**, *4*, 1384; b) P. D. Croucher, P. J. Nichols, C. L. Raston, *J. Chem. Soc. Dalton Trans.* **1999**, 279; c) P. C. Andrews, J. L. Atwood, L. J. Barbour, P. D. Croucher, P. J. Nichols, N. O. Smith, B. W. Skelton, A. H. White, C. L. Raston, *J. Chem. Soc. Dalton Trans.* **1999**, 2927; d) P. D. Croucher, J. M. E. Marshall, P. J. Nichols, C. L. Raston, *Chem. Commun.* **1999**, 193.
- [16] M. M. Olmstead, D. A. Costa, K. Maitra, B. C. Noll, S. L. Phillips, P. M. Van Calcar, A. L. Balch, *J. Am. Chem. Soc.* **1999**, *121*, 7090.
- [17] D. H. Hochmuth, S. L. J. Michel, A. J. P. White, D. J. Williams, A. G. M. Barrett, B. M. Hoffman, *Eur. J. Inorg. Chem.* **2000**, 593.
- [18] a) P. D. W. Boyd, M. C. Hodgson, C. E. F. Rickard, A. G. Oliver, L. Chaker, P. J. Brothers, R. D. Bolskar, F. S. Tham, C. A. Reed, *J. Am. Chem. Soc.* **1999**, *121*, 10487; b) D. R. Evans, N. L. P. Fackler, Z. Xie, C. E. F. Rickard, P. D. W. Boyd, C. A. Reed, *J. Am. Chem. Soc.* **1999**, *121*, 8466.
- [19] S. Stevenson, G. Rice, T. Glass, K. Harich, F. Cromer, M. R. Jordan, J. Craft, E. Hadju, R. Bible, M. M. Olmstead, K. Maitra, A. J. Fisher, A. L. Balch, H. C. Dorn, *Nature* **1999**, *401*, 55.
- [20] E. I. Yudanov, D. V. Konarev, L. L. Gumanov, R. N. Lyubovskaya, *Russ. Chem. Bull.* **1999**, *48*, 718.
- [21] a) Yu. V. Zefirov, P. M. Zorkii, *Russ. Chem. Rev.* **1995**, *64*, 415; b) R. S. Rowland, R. Taylor, *J. Phys. Chem.* **1996**, *100*, 7384.
- [22] J. H. Williams, *Acc. Chem. Res.* **1993**, *26*, 593.
- [23] H.-B. Burgi, E. Blanc, D. Schwarzenbach, S. Liu, Y.-J. Lu, M. M. Kappes, J. A. Ibers, *Angew. Chem.* **1992**, *104*, 667; *Angew. Chem. Int. Ed. Engl.* **1992**, *31*, 640.
- [24] F. H. Allen, O. Kennard, *Chem. Des. Autom. News* **1993**, *8*, 31.
- [25] U. Bilow, M. Jansen, *J. Chem. Soc. Chem. Commun.* **1994**, 403.
- [26] A. L. Balch, M. M. Olmstead, *Chem. Rev.* **1998**, *98*, 2123.
- [27] a) K. Hedberg, L. Hedberg, D. S. Bethune, C. A. Brown, H. C. Dorn, R. D. Johnson, M. DeVries, *Science* **1991**, *254*, 410; b) G. Roth, P. Adelmant, *J. Phys. I* **1992**, *2*, 1541.
- [28] M. J. Hamor, T. A. Hamor, and J. L. Hoard, *J. Am. Chem. Soc.* **1964**, *86*, 1938.
- [29] M. P. Byrn, C. J. Curtis, S. I. Khan, P. A. Sawin, R. Tsurumi, C. E. Strouse, *J. Am. Chem. Soc.* **1990**, *112*, 1865.
- [30] B. Cheng, O. Q. Munro, H. M. Marques, W. R. Scheidt, *J. Am. Chem. Soc.* **1997**, *119*, 10732.
- [31] E. B. Fleischer, C. K. Miller, L. E. Webb, *J. Am. Chem. Soc.* **1964**, *86*, 2342.
- [32] M. P. Byrn, C. J. Curtis, I. Goldberg, Yu. Hsiou, S. I. Khan, P. A. Sawin, S. K. Tendick, C. E. Strouse, *J. Am. Chem. Soc.* **1991**, *113*, 6549.
- [33] a) J. Stankowski, P. Byszewski, W. Kempinski, Z. Trybuka, N. Zuk, *Phys. Status Solidi B* **1993**, *178*, 221; b) M. D. Pace, T. C. Christidis, J. J. Yin, J. Millikin, *Phys. Chem.* **1992**, *96*, 6858; c) P. Paul, R. D. Bolskar, A. M. Clark, C. A. Reed, *Chem. Commun.* **2000**, 1229.
- [34] B. Wayland, L. W. Olson, Z. U. Siddiqui, *J. Am. Chem. Soc.* **1976**, *98*, 94.
- [35] J. M. Assour, *J. Chem. Phys.* **1965**, *43*, 2477.
- [36] a) T. Picher, R. Winkler, H. Kuzmany, *Phys. Rev. B* **1994**, *49*, 15879; b) V. N. Semkin, N. V. Drichko, A. V. Talysin, A. Graja, S. Krol, D. V. Konarev, R. N. Lyubovskaya, *Synth. Met.* **1998**, *93*, 207.
- [37] Yu. M. Shul'ga, V. I. Rubtsov, A. S. Lobach, *Z. Phys. B* **1994**, *93*, 327.
- [38] A. Wolberg, J. Manassen, *J. Am. Chem. Soc.* **1970**, *92*, 2982.
- [39] D. Dubois, K. M. Kadish, S. Flanagan, R. F. Haufler, L. P. F. Chibante, L. J. Wilson, *J. Am. Chem. Soc.* **1991**, *113*, 4364.
- [40] K. Nagai, T. Iyoda, K. Hashimoto, A. Fujishima, *Abstracts of Papers, International Conference on Perspectives in Organic–Inorganic Hybrid Solids, Nagoya (Japan)*, **1996**, p. 118.
- [41] H. B. Bürgi, R. Restori, D. Schwarzenbach, A. L. Balch, J. W. Lee, B. C. Noll, M. M. Olmstead, *Chem. Mater.* **1994**, *6*, 1325.
- [42] S. A. Reed, J. K. Kouba, C. J. Grimes, S. K. Cheung, *Inorg. Chem.* **1978**, *17*, 2666.
- [43] *SMART and SAINT, Area detector control and integration software, Ver. 6.01*, Bruker Analytical X-ray Systems, Madison, WI (USA), **1999**.
- [44] *SHELXTL, An integrated system for solving, refining and displaying crystal structures from diffraction data, Ver. 5.10*, Bruker Analytical X-ray Systems, Madison, WI, (USA) **1997**.

Received: July 31, 2000

Revised: February 16, 2001 [F2636]